

On The Estimation of Dynamic Rupture Parameters

S. Peyrat⁽¹⁾, K.B. Olsen⁽¹⁾, and R. Madariaga⁽²⁾

(1) Institute for Crustal Studies, University of California, Santa Barbara, USA (e-mail: peyrat@crustal.ucsb.edu, kbolsen@crustal.ucsb.edu; phone: 805 893 2820, 805 893 7394, fax: 805 893 8649). (2) Laboratoire de Géologie, Ecole Normale Supérieure, 24 rue Lhomond, 75231 Paris Cedex 05, France (email: madariag@geophy.ens.fr; phone: +33 1 44 32 22 16; fax: +33 1 44 32 22 00.)

Abstract

We have tested to which extent commonly-used dynamic rupture parameters can be resolved for a realistic earthquake scenario from all available observations. For this purpose we have generated three dynamic models of the Landers earthquake using a single, vertical, planar fault segment with heterogeneity of *either* the initial stress, the yield stress, or the slip-weakening friction. Although the dynamic parameters for these models are inherently different, all the simulations are in agreement with strong motion, GPS, InSAR, and field data for the event. The rupture propagation and slip distributions obtained for each model are similar, thus we have showed that the solution of the dynamic problem is non-unique. In other words, it may not be possible to separate strength drop and D_c using rupture modeling, in agreement with the results by Gattereri and Spudich (2000) [7].

Rupture Inversion

The M 7.3 June 28 1992, Landers earthquake is one of the largest, most well-recorded earthquakes in California. It occurred in the Mojave Desert in southern California on a series of right-lateral strike-slip faults within the Eastern California Shear Zone. The high quality and variety of data available for this event provided an unprecedented opportunity to study its kinematic rupture process in detail. In a first attempt at constructing a dynamic model of the Landers earthquake, Olsen et al. (1997) [5] studied the frictional conditions under which rupture could propagate and then modeled the dynamic rupture process for the initial stress field obtained from the slip distribution determined by [8].

Peyrat et al. (2001) [6] carried the initial study by Olsen et al. (1997) [5] a step further by inverting for the initial conditions on the fault using the observed ground motion. By trial-and-error inversion of strong motion data Peyrat et al. (2001) found an asperity model (variable initial stress) and a barrier model (variable yield stress T_u) (Figure 1a-b) for the Landers rupture. Here, we present an additional barrier model, with variable slip-weakening distance D_c , from trial-and-error inversion (Figure 1c). Thus we have computed three well-posed mechanical models of the rupture propagation which satisfy observed accelerograms. For the barrier models the starting models for the inversion were estimated using the parameter $\kappa = T_e^2 W / \mu (T_u - T_f) D_c$, a nondimensional parameter identified by Madariaga and Olsen (2000) [2].

In order to test the resolution of InSAR and GPS data to constrain rupture parameters, we computed the three-component area-wide distribution of ground displacement (Figure 2a-c) from the slip distribution (Figure 1a-c) for our three dynamic rupture models using Okada's (1985) [4] formulation. For comparison we have modeled a constant slip distribution, equivalent to the mean of the slip generated by the asperity model (Figure 2d) and the slip distribution of the asperity model projected on three segments (Figure 2e). The overall shape of the fringes are well reproduced by our models (Figures 2a-c), while a direct comparison is difficult because of the curvature of the fault (we use only one segment in our dynamic simulations). The three-segment model (Figure 2e) shows a better fit with data than that for the same slip distribution with only one segment (Figure 2a). The agreement between the three-segment synthetic and observed interferograms is satisfactory except for the effects of the M 6.2 Big Bear event which occurred the same day as the Landers earthquake and which were not included in the model. Thus, InSAR data provide a constraint on the geometry of the fault. Furthermore, the shape and amplitude of the fringes for the synthetic interferograms from a constant slip distribution (Figure 2d) are much smoother and smaller, respectively, compared to those generated by the more realistic heterogeneous model. Therefore, the modeling of SAR interferograms provides a constraint on the spatial variation of the slip distribution. We find the same conclusions from similar modeling of horizontal GPS data (Figure 3).

The three models are in agreement with InSAR (Figure 2), GPS (Figure 3) and field data for the event, and provide a very satisfactory fit between synthetic and strong motion data (Figure 4). The rupture histories from the three dynamic inversion models (Figure 5) are in good agreement with that from the kinematic inversion results of Wald and Heaton (1994) [8]. There are no major differences between the models, even though the initial conditions are completely different.

Discussion and Conclusions

Three well-posed mechanical models, an asperity and two barrier models, have been constructed of the Landers event, that generate synthetics in agreement with strong motion, GPS, InSAR, and field data. There are no major differences between the models, even though the initial conditions, and therefore their physical interpretation, are completely different. The three models are end-members of a large family of dynamically correct models, and the rupture for the Landers earthquake is likely a combination of these models, as intuitively, all the parameters must be heterogeneous. Thus we have showed that the solution of the dynamic problem is not unique, and it may not be possible to separate strength drop and D_c using rupture modeling with current bandwidth limitations, in agreement with Guatteri and Spudich (2000) [7]. However, prospects for including higher frequencies from near-field records of large earthquakes may enable such inversion in the future.

Acknowledgments

The computations in this study were partly carried out on the SUN Enterprise at MRL/ICS, UCSB with support from the Southern California Earthquake Center (SCEC), USC 572726 through the NSF cooperative agreement EAR-8920136.

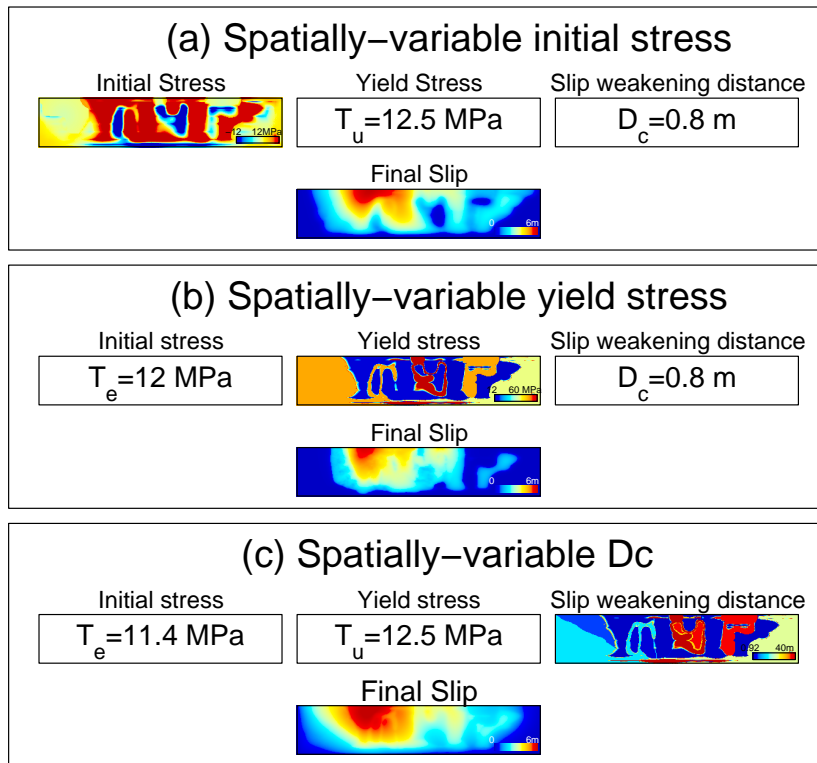


Figure 1: Initial conditions and final slip distribution on the fault for (a) the asperity model (spatially-variable initial stress), (b) the barrier model with spatially-variable yield stress, and (c) the barrier model with spatially-variable D_c .

References

- [1] Madariaga, R., Olsen, K.B., and Archuleta, R., 1998, *Modeling Dynamic Rupture in a 3D Earthquake Fault Model*, Bull. Seism. Soc. Am., **88**, 1182-1197.
- [2] Madariaga, R., and Olsen, K.B., 2000, *Criticality of rupture dynamics in 3-D*, Pure Appl. Geophys., **157**, 1981-2001.
- [3] Massonnet, D., Rossi, M., Carmona, C., Adragna, F., Peltzer, G., Feigl, K., and Rabaute, T., 1993, *The displacement field of the Landers earthquake mapped by radar interferometry*, Nature, **364**, 138-142.
- [4] Okada, Y., 1985, *Surface deformation due to shear and tensile faults in a half-space*, Bull. Seismol. Soc. Am., **75**, 1135-1154.
- [5] Olsen, K.B., Madariaga, R., and Archuleta, R., 1997, *Three dimensional dynamic simulation of the 1992 Landers earthquake*, Science, **278**, 834-838.
- [6] Peyrat, S., Olsen, K., and Madariaga, R., 2001, *Dynamic modeling of the 1992 Landers earthquake*, J. Geophys. Res., **106**, 26,467-26,482.
- [7] Guatteri, M. and Spudich, P., 2000, *What can strong-motion data tell us about slip-weakening fault-friction laws?*, Bull. Seis. Soc. Am., **90**, 98-116.

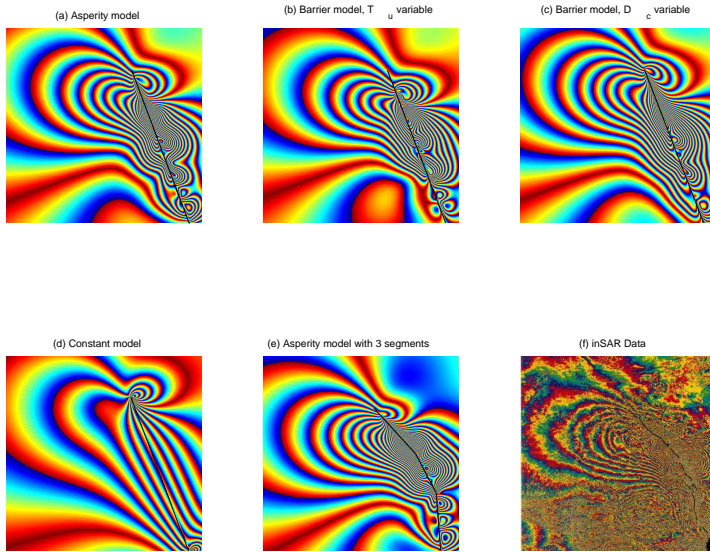


Figure 2: (a-e) Synthetic interferograms calculated on a rectangular grid with 200 m spacing for the Landers earthquake. (f) Observed coseismic interferogram cover a 90 by 110 km area from April 24 to August 7, 1992 (Massonnet et al., 1993) [3]. Each cycle of interferogram colors (red to blue) represents 28 mm of ground motion in the direction of the satellite. Black segments depict the fault geometry for each model.

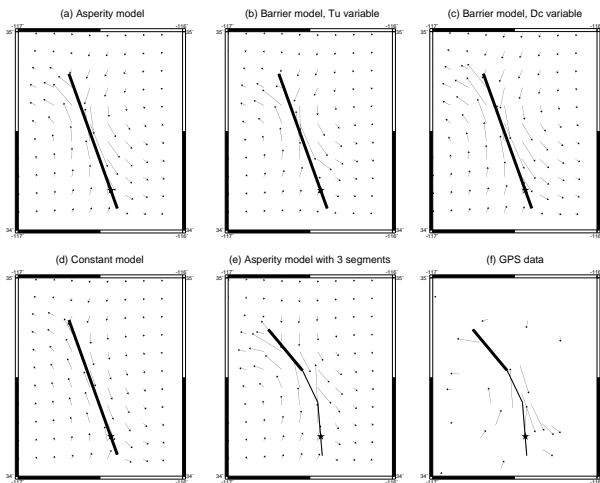


Figure 3: (a-e) Predicted horizontal GPS displacements calculated for the Landers earthquake depicted by arrows on a regular grid. (f) Observed horizontal displacements at GPS stations.

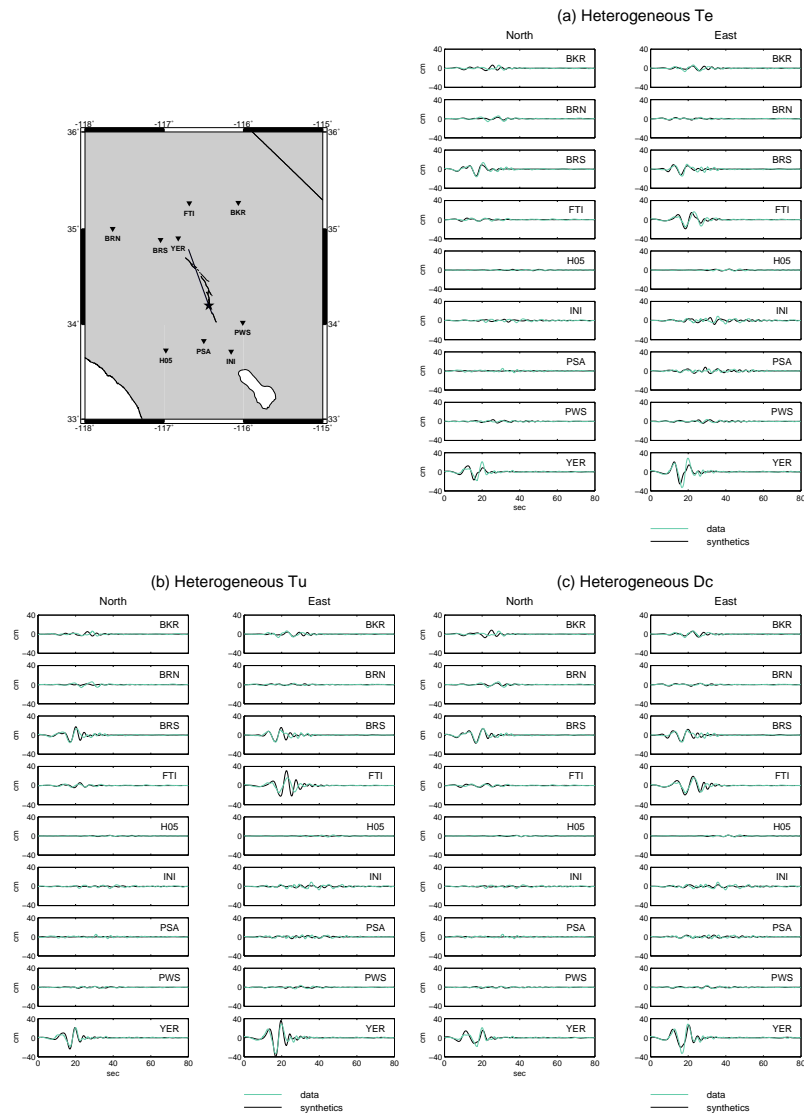


Figure 4: Comparison between observed ground displacements (black) and those obtained for our inverted dynamic models of the 1992 Landers earthquake (green). The overall waveforms are well reproduced by the synthetics.

[8] Wald, D., and Heaton, T., 1994, *Spatial and temporal distribution of slip for the 1992 Landers, California, earthquake*, Bull. Seismol. Soc. Am., **84**, 668-691.

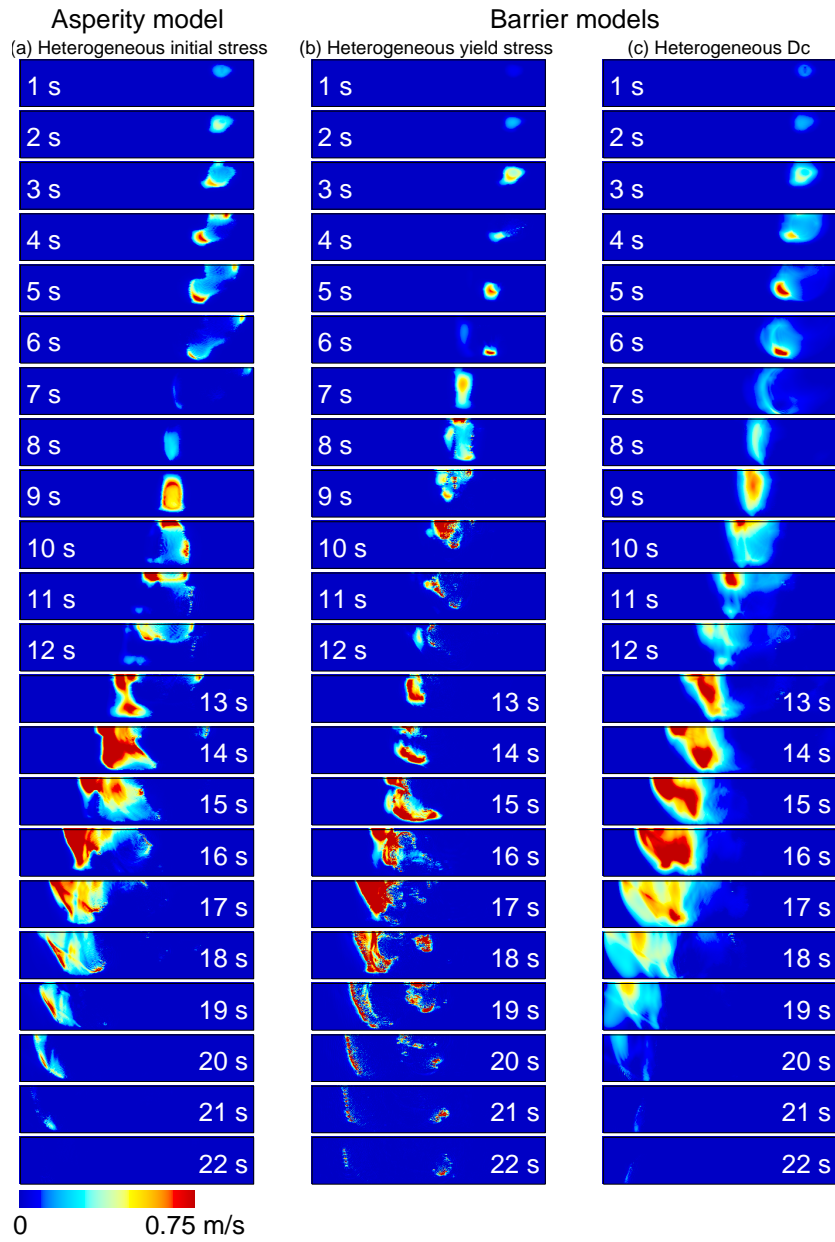


Figure 5: Rupture history for the three complementary models of the Landers earthquake. Each snapshot depicts the horizontal sliprate on the fault during 1 s time slice. The rupture propagates along a complex path, and shows a confined band of slip propagating unilaterally towards the northwest.